engineering proceedings

MDPI

Proceeding Paper

Optical Detection of Cerium (Ce^{3+}/Ce^{4+}) Ions in Microparticles of Yttrium–Aluminum Garnet Powder (YAG:Ce^{3+})-Embedded Free-Standing Composite Films for Narrowband Blue to Broadband Visible Light Downconversion †

Denys N. Khmil *, Irina E. Minakova, Vladimir S. Kretulis, Pavlo O. Tytarenko, Alexandr M. Kamuz and Borys A. Snopok

Department of Optoelectronics, V.E. Lashkaryov Institute of Semiconductor Physics, National Academy of Sciences of Ukraine, 41 Pr. Nauki, 03028 Kyiv, Ukraine; minakova@isp.kiev.ua (I.E.M.); kretulis@isp.kiev.ua (V.S.K.); tytarenko@isp.kiev.ua (P.O.T.); kamuz@isp.kiev.ua (A.M.K.); snopok@isp.kiev.ua (B.A.S.)

* Correspondence: khmil@isp.kiev.ua

† Presented at The 11th International Electronic Conference on Sensors and Applications (ECSA-11), 26–28 November 2024; Available online: https://sciforum.net/event/ecsa-11.

Abstract: A method for measuring light intensity at different depths of a strongly scattering medium (composite films of photoluminophore YAG:Ce^{3+}) has been developed. The depth at which a collimated light source is converted into an isotropic radiation source was determined. The volumetric absorption coefficient of luminophore powder microparticles, which are suspended in the suspension, was measured. The concentration of trivalent cerium ions (Ce^{3+}) in the powder particles of composite films was determined. It is shown for the first time that bulk light absorption increases the number of absorbed light quanta in a particle by a factor of six, without increasing the concentration of cerium ions in the particle.

Keywords: turbid media; composite films; optoelectronic step-down convertors; light absorption coefficient; yttrium–aluminum garnet; phosphors; white LED

check for updates

Citation: Khmil, D.N.; Minakova, I.E.; Kretulis, V.S.; Tytarenko, P.O.; Kamuz, A.M.; Snopok, B.A. Optical Detection of Cerium (Ce^{3+}/Ce^{4+}) Ions in Microparticles of Yttrium–Aluminum Garnet Powder (YAG:Ce^{3+})-Embedded Free-Standing Composite Films for Narrowband Blue to Broadband Visible Light Downconversion. *Eng. Proc.* **2024**, *82*, 81. https://doi.org/10.3390/ecsa-11-20356

Academic Editor: Jean-marc Laheurte

Published: 25 November 2024

1. Introduction

The search for more efficient ways to create both light sensors and VIS-IR sources has led to an ever-growing interest in coatings that convert UV radiation into white light. GaN LEDs with an emission wavelength of about 460 nm are most often used as UV emitters.

Step-down UV-converters are often made from suspensions of rare-earth phosphor powders (e.g., cerium-activated yttrium–aluminum garnets—YAG:Ce^{3+}) for the transformation of narrowband blue radiation into broadband VIS luminescent emission (540–590 nm). Depending on the technological process, the concentrations of trivalent Ce^{3+} ions and tetravalent Ce^{4+} ions in the yttrium—aluminum garnet matrix change significantly. It is obvious that improving production technology is impossible without promptly measuring the concentration of Ce^{3+} ions in the transparent matrix, depending on the technological conditions of the synthesis.

The difficulty of experimentally determining the optical characteristics of films of optoelectronic converters is related to the fact that the phosphor composite is a classical turbid medium. Until now, in turbid media, it is impossible to simply measure their most important optical parameters; when a light wave propagates in a turbid medium, its intensity gradually decreases due to scattering and absorption, and its contribution to the extinction of light cannot be separated. Previously [1,2], we considered an original model approach and optimized the composite production protocol to overcome ambiguity in experimental measurements, which makes it possible to determine the absorption of microcrystals in a phosphor-resin composition from the measured values of the transmittance of a set of films in a certain range of thicknesses.

In this report, we examine an optical approach and technological features that allows engineers to directly optimize the emission performance of optoelectronic UV downconverters for yttrium–aluminum garnet powder doped with trivalent cerium (Ce^{3+}), taking into account the turbidity of composite films.

2. Materials and Methods

2.1. Production of Photoluminophore Powder Suspension

Suspensions were prepared as follows. Photoluminescent powder with a mass concentration of C = 0.2 was added to the epoxy resin. The suspension was carefully degassed and homogenized.

We have developed our own method for preparing a photoluminophore suspension using a forvacuum unit and have tested the technique on different types of binders (epoxy resin, silicone, and polymethyl methacrylate). Experimental studies have shown that we obtain the best results when using epoxy resin as a binder.

A suspension of photoluminophores was prepared using a turbine micromixer in a vacuum chamber, with the simultaneous homogenization and degassing of the suspension. The degassing process was visually monitored through the window of the vacuum chamber to record the time when the separation ("boiling") of gas bubbles from the suspension completely stopped. From such a degassed and homogenized suspension, plane-parallel samples of composite films were prepared. Studies of the homogeneity of the samples were carried out by determining the colorimetric characteristics in different parts of the film sample using a high-precision HAAS-2000 array spectroradiometer and an Edison EDSB 3LA1-1 blue LED with a maximum radiation of 456 nm. Colorimetric studies of composite films showed that color coordinates and correlated color temperature had very small error values of X = ±0.002, Y = ±0.003 and ±50 K, respectively. We measured the light absorption coefficient of photoluminophore microparticles at these error values of the suspension's colorimetric parameters.

2.2. Production of Samples in the Form of Plane-Parallel Films of Precision Thickness

For the manufacture of plane-parallel films, a suspension was used that was prepared from the materials specified in Section 2.1.

The essence of the manufacturing method is that spacers were applied to the laboratory glass, which set the precision thickness of the film from 50 to 500 microns. Between the spacers, a small amount of prepared photoluminophore suspension was applied, pressed on top by a second laboratory glass. Such a workpiece was placed in a specially designed and manufactured mechanism, where it was clamped with a force equal to 5 N.

Plane-parallel samples of composite films, which were made from a homogenized and degassed phosphor suspension, had precision thicknesses equal to 110, 140, 205, 255, 305, 310, 350, 410, 450, 485 and 495 μm.

Measurements of the light absorption coefficient of photoluminophore powder microparticles were carried out on an optical unit designed on the basis of the Standa holographic table with a full set of accessories and a high-precision HAAS-2000 matrix spectroradiometer [3,4].

3. Results and Discussion

3.1. Propagation of Light in Turbid Media with Multiple Photon Scattering

Turbid media are characterized [5] by such optical parameters as the absorption coefficient μ_a, scattering coefficient μ_s, extinction coefficient k_λ and anisotropy parameter g, while $k_\lambda = \mu_a + \mu_s$.

The transport free path length of a photon is defined as $l_{tr} = \frac{1}{\mu_a + \mu_s * (1-g)}$ (Figure 1). The transport free path l_{tr} is the distance at which a photon completely loses its original direction. Figure 1 schematically shows the transport free path l_{tr} and the photon free path length l_{ph}. It can be seen that the transport length of the free path of a photon in a medium

with anisotropic single scattering is significantly greater than the free path of a photon $l_{tr} >> l_{ph}$.

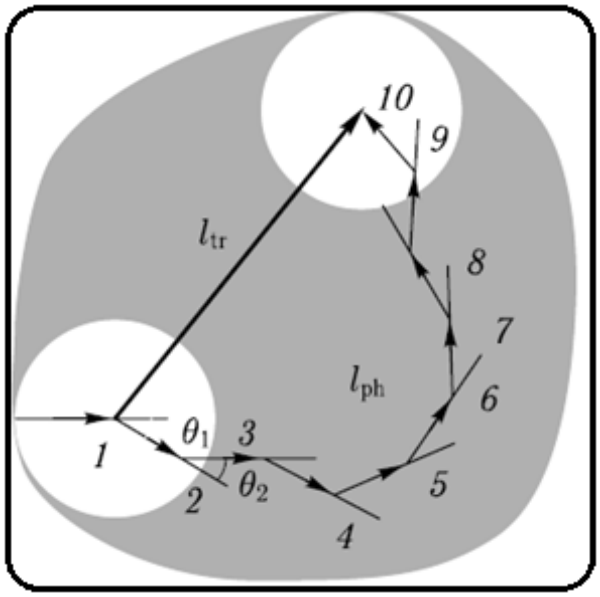

Figure 1. Determination of the transport length of the free path of a photon under multiple scattering. The average path of the photon's trajectory after its interaction with scattering particles is shown (only the first and last particles are shown in the form of light circles; small arrows (1–10) show the path of photon migration; the large arrow shows the resulting direction of photon transport as a result of multiple scattering).

In [6–9], it was shown that a collimated light source, when moving in a strongly scattering medium, is always transformed into an isotropic point radiation source with $g = 0$, which is located at a distance of one average transport length of the photon's free path $l'_{tr} = \frac{1}{\mu_a+\mu_s} \approx \frac{1}{\mu s}$ from the surface of a strongly scattering medium.

3.2. Method for Measuring Light Intensity at Different Depths of a Strongly Scattering Medium

Earlier, we showed [1,2] that in a turbid medium, it is possible to separately study both the mechanism of light scattering and absorption, as well as only one absorption mechanism. For this purpose, it is necessary to measure the distribution of light intensity inside the film along its depth. The technique of such a measurement is described in detail in [1,2]. Briefly, the essence of the technique is that the Bouguer–Lambert law must be written in a form that uses the light intensities at the points that are inside the sample. The Bouguer–Lambert law is simplified (there is no reflection coefficient from the interface between the two media) and it has the following form: $\frac{I_{1i}(d_1)}{I_{0i}} = exp(-k_\lambda * d_1)$. Here, I_{0i} is the intensity of light at the beginning of the absorbing medium (immediately after the interface) and $I_{1i}(d_1)$ is the intensity of light at the end of the sample with a thickness d_1 (before the interface).

Eleven plane-parallel samples of composite films of different thicknesses were made from the same batch of homogenized and degassed suspension. Then, the light intensity $I_1, \ldots, I_{11}$ at the exit of the samples with thickness $d_1, \ldots, d_{11}$ was sequentially measured when light with intensity I_0 was applied to their inputs; taking into account the reflection coefficients from the interface of the media (film–air), the intensities I_{0i}, $I_{1i}(d_1), \ldots, I_{11i}(d_{11})$ were determined. It is obvious that the intensities of light at the beginning of the scattering and absorbing medium in all samples have the same values, equal to I_{0i}, and the intensities at the end of the scattering and absorbing media are, respectively, equal to $I_{1i}(d_1), \ldots, I_{11i}(d_{11})$. For example, Figure 2 shows how the intensity $I_{1i}(d_1)$ was determined in a sample with a thickness d_{11}. Samples with thicknesses d_1 and d_{11} were located

next to each other and light beams with the same intensities I_0 were supplied to inputs. It is clear that inside each of the samples, there will be beams of light with the same intensities, equal to I_{0i} (blue lines in both samples). The intensity of light before leaving the sample with thickness d_1 will be equal to $I_{1i}(d_1)$ (shown in Figure 2 with a light blue arrow). The same intensity $I_{1i}(d_1)$ will be created in a sample with a thickness d_{11} at a distance d_1 from the input end (the blue lines show the positions of the intensities $I_{1i}(d_1)$ in both samples).

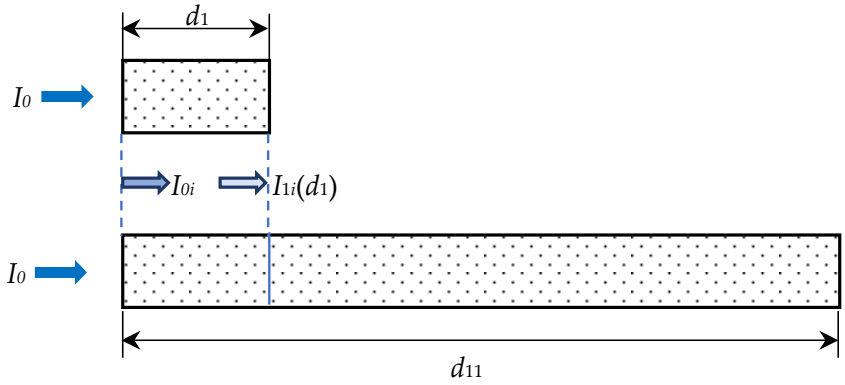

Figure 2. Determination of the location of light intensities $I_{1i}(d_1), \ldots I_{11i}(d_{11})$ in a sample with thickness d_{11}.

Placing the samples with thickness d_{11} and with thickness $d_2, \ldots d_{10}$ in pairs in the same way, we determine the location of intensities $I_{2i}(d_2), \ldots I_{10i}(d_{10})$ in the sample with thickness d_{11}.

Using the values I_{0i}, $I_{1i}(d_2)$, $I_{2i}(d_2), \ldots I_{11i}(d_{11})$, we determine the extinctions (attenuations) of light intensity $ln\left(\frac{I_{Ni}(d_N)}{I_{0i}}\right)$, as well as $ln(I_{Ni})$, for samples with thicknesses d_N, $N = 1, \ldots, 11$ (Figure 3).

From Figure 3, it can be seen that the extinction graph (1) has two slopes with the values of angles $\Theta_1 = -47.53^\circ$ and $\Theta_2 = -25.80^\circ$; with an increase in the thickness of the sample, the angle of inclination changes abruptly (the point of "break" of the slope is at a thickness of 0.0278 cm).

Since the angle of inclination of the extinction graph is proportional to the extinction coefficient, this means that before the breaking point, the extinction coefficient is equal to $-k_\lambda = -(\mu_s + \mu_a)$, and after the breaking point, the extinction coefficient abruptly decreases to the value of $-k_\lambda = -\mu_a$.

Thus, the abrupt change in light intensity inside the sample (and, accordingly, the logarithm of light intensity) is the root cause of the change in the slope of the extinction graph (1). This means that inside the sample, there is a process of changing the mechanism of the interaction of light with turbid medium. At sample thicknesses smaller than H_t (Figure 3), anisotropic scattering and the absorption of light (layer 1) occurs, and at sample thicknesses larger than H_t, the isotropic absorption of light occurs (layer 2).

As the beam moves in layer 1, the scattering anisotropy parameter g gradually decreases from +1 to 0. At the same time, the flux of photons that move along the optical axis of the measuring module in the solid angle Ω and enter the fiberoptic cable of the spectroradiometer decreases [3,4]. That is, in layer 1, there is a change in light intensity due to both anisotropic scattering and light absorption. A different picture is observed in layer 2. In layer 2, there is an isotropic scattering of light ($g = 0$), in which the same number of photons moves in any direction in the elementary solid angle, i.e., isotropic scattering does not change the number of photons that move along the optical axis of the measuring circuit in solid angle Ω and enter the fiberoptic cable. In layer 2, the number of photons changes only due to absorption and the measurement of the volume absorption coefficient can be performed only in layer 2.

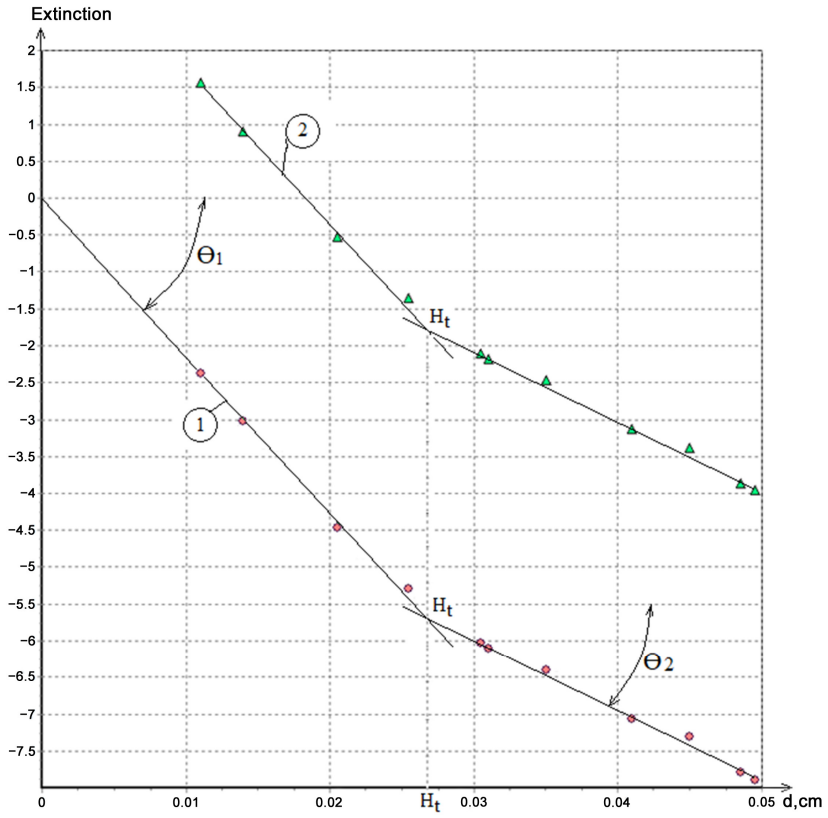

Figure 3. Extinction plot $ln\left(\frac{I_{Ni}(d_N)}{I_{0i}}\right)$ (1) and $ln(I_{Ni})$ plot (2) at points with thickness values $d_1, \ldots, d_{11}$.

3.3. Method for Measuring the Volume Absorption Coefficient of Microparticles of Photoluminophore Powder YAG:Ce^{3+} in Composite Films

We model the composite film made of suspension using phosphor cubes [1,2] with edge sizes from 1 to 10 μm. Let us consider the process of light absorption via phosphor cubes in suspension, taking into account the results of [10–14].

In the case of anisotropic light scattering in composite films, light enters the microparticle mainly through only one entrance surface (in layer 1). The absorption of the particle is characterized by a linear absorption coefficient $_{\lambda p}$. In the case of isotropic light scattering in composite films, light enters each microparticle of layer 2 through all six faces of the cube. The absorption of the particle is characterized by the volumetric absorption coefficient $_{\lambda}$.

Our numerous measurements of the absorption coefficients of YAG:Ce^{3+} photoluminophore microparticles have shown that the estimated ratio $ß_{\lambda p} = \frac{ß_{\lambda}}{6}$ is always fulfilled for the linear absorption coefficient $ß_{\lambda p}$.

The estimated value of the linear light absorption coefficient $ß_{\lambda p}$ of one microparticle at a wavelength of 456 nm is 129 cm^{-1}.

3.4. Measurement of the Concentration of Trivalent Ce^{3+} Ions in a Microparticle of YAG:Ce Phosphor Powder

The authors of [15] determined the absorption cross-section σ of one Ce^{3+} ion using the standard formula $\sigma = \frac{\alpha_{\lambda}}{N}$, where α_{λ} is the linear absorption coefficient of the single crystal and N is the concentration of Ce in atoms/cm^3. Since the analytical relationship between the linear absorption coefficient of an yttrium–aluminum garnet single crystal YAG:Ce^{3+} and the concentration of Ce^{3+} ions in it does not depend on the size of the single crystal; the ratio $\sigma = \frac{ß_{\lambda p}}{N}$ is also held in a single-crystal particle of photoluminophore powder YAG:Ce^{3+}, where $ß_{\lambda p}$ is the linear absorption coefficient of the microparticle of the photoluminophore powder (particle size is $1 \div 20$ μm) [15].

The magnitude of bulk absorption depends on the concentration of microparticles in composite films. The number of scattered photons in a turbid medium is significant and, as a rule, several times higher than the number of absorbed photons. The transport free path length of a photon in a highly scattering medium significantly exceeds the photon free path length $l'_{tr} >> l_{ph}$, which leads to the fact that photons accumulate in layer 2. The speed of photon motion along the Z coordinate decreases. As a result, in a strongly scattering medium, the light energy is absorbed at a smaller distance Z than when propagating in a homogeneous medium.

At the linear absorption coefficient $ß_{\lambda p}$ of the phosphor powder particle, the concentration N of trivalent Ce^{3+} ions in the particle is [15] $N = \frac{ß_{\lambda p}}{\sigma} = \frac{129}{3\times10^{-18}} = 0.43 \times 10^{20}$ [ions/cm^3].

Since the volume absorption coefficient $ß_{\lambda}$ of the phosphor powder particle is six times larger than the linear absorption coefficient $ß_{\lambda p}$, the effective concentration N_{ef} of trivalent Ce^{3+} ions in the microparticle increases six times, i.e., $N_{ef} = 0.28 \times 10^{21}$ [ions/cm^3]. This means that the same cerium ions in the particle take part in absorption repeatedly (6-fold). Such multiple absorption of light quanta by the same cerium ions in the particle causes the process of the bulk absorption of light in the microparticle. Thus, the bulk absorption, without increasing the concentration of cerium in the particle, increases the number of absorbed light quanta in it by a factor of 6-fold.

4. Conclusions

A method for measuring light intensity at different depths of a strongly scattering medium (composite films of YAG:Ce^{3+} photoluminophores) has been developed. The depth $H_t = l'_{tr}$ at which a collimated light source is converted into an isotropic radiation source has been determined. The volumetric absorption coefficient of the luminophore powder microparticles, which are suspended in the suspension, has been measured. The concentration of trivalent cerium ions (Ce^{3+}) in the powder particles of composite films was determined. It is shown for the first time that the bulk absorption of light $ß_{\lambda}$ by powder particles increases the effective concentration N_{ef} of trivalent Ce^{3+} ions in the microparticle by a factor of six. It is shown that bulk light absorption increases, by a factor of six, the number of absorbed light quanta in the particle without increasing the concentration of cerium ions in it.

Author Contributions: Conceptualization: B.A.S. and A.M.K.; methodology: B.A.S. and A.M.K.; validation and sample preparation: D.N.K. and P.O.T.; investigation: D.N.K., V.S.K. and I.E.M.; writing—original draft preparation: A.M.K. All authors have read and agreed to the published version of the manuscript.

Funding: This research received no external funding.

Institutional Review Board Statement: Not applicable.

Informed Consent Statement: Not applicable.

Data Availability Statement: Data are available upon request.

Conflicts of Interest: The authors declare no conflicts of interest.

References

1. Khmil, D.N.; Kamuz, A.M.; Oleksenko, P.F.; Kamuz, V.G.; Aleksenko, N.G.; Kamuz, O.A. Method for determination of the absorption coefficient in films based on photoluminophore suspension for white LEDs. *Semicond. Phys. Quantum Electron. Optoelectron.* **2015**, *18*, 215–219. [CrossRef]
2. Khmil, D.N.; Kamuz, A.M.; Oleksenko, P.F.; Kamuz, V.G.; Aleksenko, N.G.; Kamuz, O.A. Determination of the spectral dependence for the absorption coefficient of phosphor inorganic microparticles. *Semicond. Phys. Quantum Electron. Optoelectron.* **2015**, *18*, 334–340. [CrossRef]
3. Kamuz, O.M.; Khmil, D.M.; Tytarenko, P.O.; Kretulis, V.S.; Minakova, I.E.; Snopok, B.A. The methodology for determining light absorption coefficients of luminophore powder YAG:Ce^{3+} microparticles and its technological support. *Optoelectron. Semicond. Tech.* **2023**, *58*, 136–146. [CrossRef]

4. Kamuz, O.; Khmil, D.; Tytarenko, P.; Kretulis, V.; Minakova, I.; Snopok, B. Photometric Ω-module for fiber optic spectrometer: A simple tool for measuring the absorption coefficient of individual microparticles in turbid media. *Opt. Eng.* **2024**, *63*, 085104-1–085104-12. [CrossRef]
5. Jacques, S.L. Tissue Optics, Short Course 29. In Proceedings of the SPIE Photonics West Conference, San Francisco, CA, USA, 1–6 February 2020.
6. Wang, L.; Wu, H. *Biomedical Optics: Principles and Imaging*; Wiley-InterScience: Hoboken, NJ, USA, 2007; p. 376.
7. Wang, L.; Jacques, S. Hybrid model of Monte Carlo simulation and diffusion theory for light reflectance by turbid media. *J. Opt. Soc. Am.* **1993**, *10*, 1746. [CrossRef] [PubMed]
8. Gardner, C.M.; Jacques, S.L.; Welch, A.J. Light Transport in Tissue: Accurate Expressions for One-Dimensional Fluence Rate and Escape Function Based Upon Monte Carlo Simulation. *Lasers Surg. Med.* **1996**, *18*, 129–138. [CrossRef]
9. Nishankovsky, S.V.; Dan'ko, A.Y.; Puzikov, V.M.; Savvin, Y.N.; Trushkovsky, A.G.; Krivonogov, S.I. Optical and luminescence characteristics of YAG:Ce crystals grown by horizontal directed crystallization in reducing gas medium. *Funct. Mater.* **2008**, *15*, 546–549.
10. Star, W.M. Light dosimetry in vivo. *Phys. Med. Biol.* **1997**, *42*, 763–787. [CrossRef] [PubMed]
11. Star, W.M.; Wilson, B.C.; Patterson, M.C. Light delivery and dosimetry in photodynamic therapy of solid tumors. In *Photodynamic Therapy, Basic Principles and Clinical Applications*; Henderson, B.W., Dougherty, T.J., Eds.; Marcel-Dekker: New York, NY, USA, 1992; pp. 335–368.
12. Tuchin, V.V.; Utz, S.R.; Yaroslavsky, I.V. Tissue optics, light distribution and spectroscopy. *Opt. Eng.* **1994**, *33*, 3178–3188. [CrossRef]
13. Wang, L.; Zhuang, L.; Xin, H.; Huang, Y.; Wang, D. Semi-Quantitative Estimation of Ce^{3+}/Ce^{4+} Ratio in YAG:Ce^{3+} Phosphor under Different Sintering Atmosphere. *Open J. Inorg. Chem.* **2015**, *5*, 2–18. [CrossRef]
14. Barbaran, J.H.; Ghamsari, M.S.; Javaheri, I.; Baharvand, B. Growth and spectral properties of Ce^{3+}:YAG single crystal. *J. Optoelectron. Adv. Mater.* **2018**, *20*, 431–434.
15. Arjoca, S.; Víllora, E.G.; Inomata, D.; Aoki, K.; Sugahara, Y.; Shimamura, K. Temperature dependence of Ce:YAG single-crystal phosphors for high-brightness white LEDs/LDs. *Mater. Res. Express* **2015**, *2*, 055503. [CrossRef]